



Slip rate gradients along the eastern Kunlun fault

Eric Kirby,¹ Nathan Harkins,¹ Erqi Wang,² Xuhua Shi,² Chun Fan,² and Douglas Burbank³

Received 5 August 2006; revised 9 December 2006; accepted 3 January 2007; published 30 March 2007.

[1] Whether strike-slip fault systems in Eurasia accomplish eastward extrusion of Tibetan crust and lithosphere depends largely on the kinematics of deformation at the fault tip. Here we present new slip rate determinations using millennial-scale geomorphic markers from sites along the easternmost segment of the Kunlun fault in north central Tibet. This fault system represents one of the major strike-slip faults within the Indo-Asian collision zone, has been argued to exhibit uniform slip rates along much of its length, and plays a central role in models for eastward extrusion of Tibetan lithosphere. Displaced fluvial terrace risers along tributaries of the Yellow River, coupled with ¹⁴C ages of terrace material, provide constraints on slip rates over late Pleistocene to Holocene time. Results indicate that slip rates decrease systematically along the eastern ~150 km of the fault from >10 to <2 mm/yr. These data challenge the view that slip along the Kunlun fault remains uniform along the entire length of the fault and instead reveal gradients in displacement similar to those expected at fault tips. Moreover, slip along the fault appears to terminate within the thickened crust of the plateau, and therefore any extrusion of Tibetan lithosphere accomplished by slip along the Kunlun fault must be absorbed by internal deformation of the plateau surrounding the fault tip. **Citation:** Kirby, E., N. Harkins, E. Wang, X. Shi, C. Fan, and D. Burbank (2007), Slip rate gradients along the eastern Kunlun fault, *Tectonics*, 26, TC2010, doi:10.1029/2006TC002033.

1. Introduction

[2] Since the recognition that active deformation within Eurasia involves lateral displacement on major strike-slip faults oriented approximately orthogonal to the convergence vector between India and Eurasia [Molnar and Tapponnier, 1975; Tapponnier and Molnar, 1977], the relative roles of eastward transport of material along these structures versus thickening of Eurasian crust in accommodating convergence has remained contentious. Two end-member views of the kinematics of Eurasian deformation have emerged.

The first class of models envision that high slip rates along major strike-slip faults account for a large fraction of the present-day velocity field [Avouac and Tapponnier, 1993; Peltzer and Saucier, 1996] and point to rapid slip rates inferred from displaced geologic and geomorphic features [Chevalier et al., 2005b; Mériaux et al., 2004] as evidence of the significance of these structures. In contrast, a class of continuum models of the collision zone predict distributed deformation and thickening throughout the orogen, along with relatively low rates of lateral slip [England and Houseman, 1986; Houseman and England, 1993; Vilotte et al., 1986]. Such models find support in recent geodetic studies that indicate broadly distributed deformation within the Tibetan Plateau [Zhang et al., 2004] and low displacement rates along major strike-slip faults [Bendick et al., 2000; Brown et al., 2002; Wang et al., 2001; Wright et al., 2004] over decadal timescales.

[3] Although much of the debate historically has been focused on whether these fault systems exhibit high or low slip rates, whether these faults accomplish eastward extrusion of Tibet depends critically whether high slip rates are maintained along the entire length of the fault system. Studies of fault growth and scaling [e.g., Cowie and Scholz, 1992a] typically reveal systematic relationships between fault length and total displacement [Stirling et al., 1996] that imply, in the absence of interactions with other faults, displacement should decrease toward the fault tip. Few studies of slip rates along Eurasian strike-slip faults, however, have considered this possibility [Bayasgalan et al., 1999]; most kinematic models assign a single slip rate to the entire fault [e.g., Avouac and Tapponnier, 1993]. Although the Altyn Tagh fault is widely considered to terminate at its intersection with the Qilian Shan [Burchfiel et al., 1989; Tapponnier et al., 2001], implying that displacement must decrease along strike [cf. Meyer et al., 1996; Mériaux et al., 2005; cf. P. Zhang et al., Late Quaternary and present-day rates of slip along the Altyn Tagh fault, submitted to *Tectonics*, 2006, hereinafter referred to as Zhang et al., submitted manuscript, 2006], this transform-like behavior is largely dictated by the fact that the Altyn Tagh fault separates deforming regions of Tibet from relatively undeformed lithosphere of the Tarim basin. Whether such behavior is characteristic of faults within the Tibetan Plateau remains unknown.

[4] A critical test of competing models for the role of strike-slip faults in the Indo-Eurasian collision may be conducted by ascertaining to what degree lateral displacement along fault systems in Tibet is accommodated by structures beyond the eastern margin of the plateau. With its great length (~1500 km), high slip rate (~10 mm/yr) [Li et al., 2005; Van der Woerd et al., 1998, 2000, 2002b], and recent seismicity [Lin et al., 2002; Van der Woerd et al., 2002a],

¹Department of Geosciences, Pennsylvania State University, University Park, Pennsylvania, USA.

²Institute for Geology, Chinese Academy of Sciences, Beijing, China.

³Department of Earth Science, University of California, Santa Barbara, California, USA.

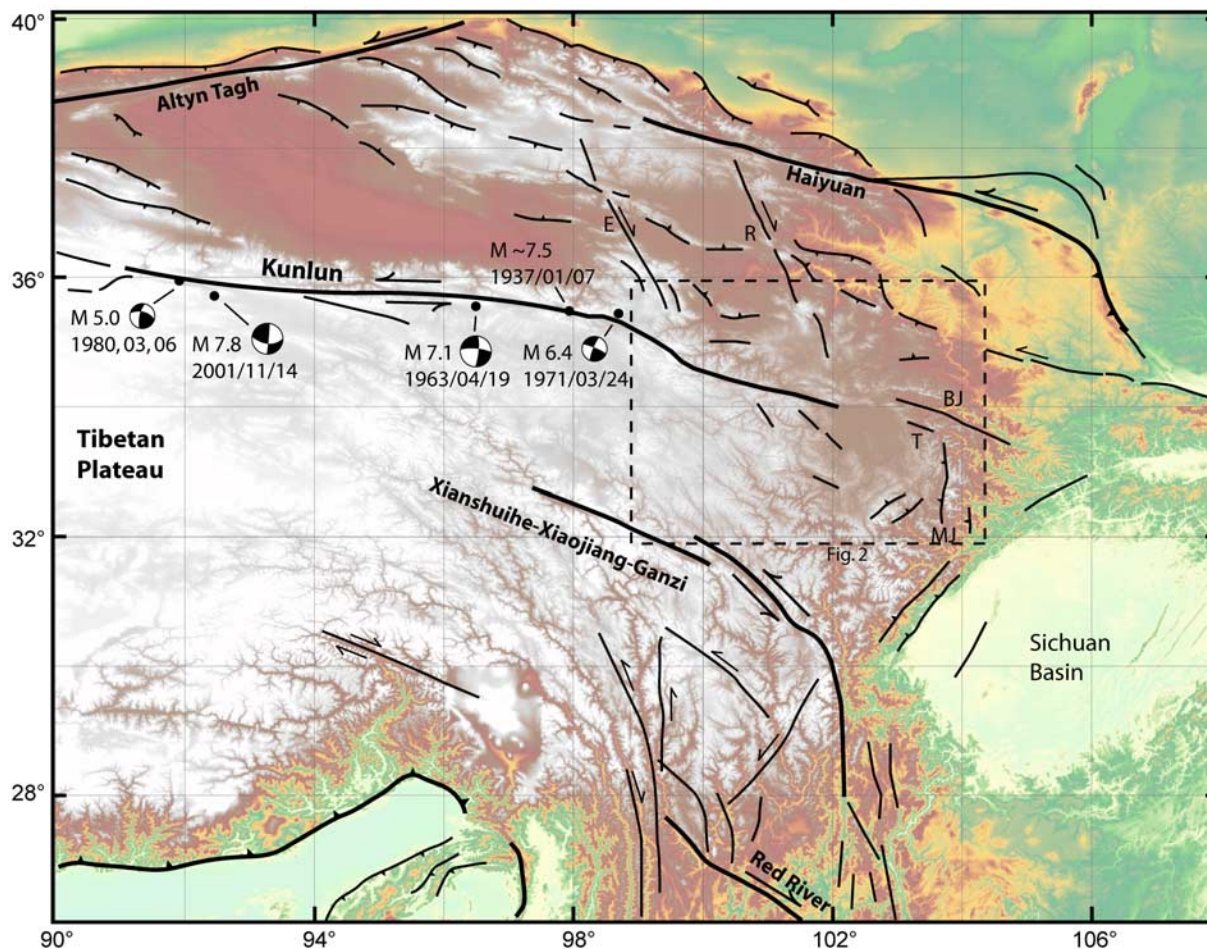


Figure 1. Tectonic map showing major and minor active faults in eastern Tibet. Abbreviations are as follows; BJ, Bailong Jiang fault; E, Elashan fault; MJ, Min Jiang fault; R, Riyueshan fault; T, Tazang fault. Epicentral locations and focal mechanism solutions of recent seismicity along the Kunlun fault are compiled from USGS (http://neic.usgs.gov/neis/epic/epic_circ.html), Harvard CMT catalog (<http://www.globalcmt.org/CMTsearch.html>), and *Molnar and Lyon-Caen* [1989]. Topographic base is generated from the Shuttle Radar Topography Mission (SRTM) data.

the Kunlun fault in north central Tibet (Figure 1) appears well suited to such a test. Unlike the Altyn Tagh fault system, the Kunlun fault separates two actively deforming regions of the plateau. Moreover, recent geologic studies suggest that millennial-scale slip rates are spatially uniform along nearly ~ 800 km of the central portion of the fault [*Li et al.*, 2005; *Van der Woerd et al.*, 1998, 2000, 2002b]. Regional geodetic estimates of the present velocity field [*Zhang et al.*, 2004] are consistent with geologic slip rates. These geodetic measurements, however, resolve little left-lateral shear [*Chen et al.*, 2000; *Zhang et al.*, 2004] across the inferred trace of the easternmost segment of the fault (east of $\sim 100^\circ\text{E}$) and suggest that the fault may terminate within the plateau.

[5] Here we report new slip rate estimates derived from displaced fluvial terrace risers along the eastern Kunlun fault. Our use of millennial-scale geomorphic features to reconstruct fault displacement is motivated by the wide-

spread distribution of these landforms, which afford opportunity to examine multiple sites and thus test for potential gradients in displacement. Moreover, the generation and abandonment of fluvial terraces appears to be synchronous in this region of Asia since the late Pleistocene [e.g., *Hetzel et al.*, 2002; *Van der Woerd et al.*, 2002b], allowing for slip rate determinations that average displacement across multiple seismic cycles, yet are relatively isochronous among different sites. We compare our slip rate determinations with those determined for similar time intervals along the central and western segments of the fault [*Li et al.*, 2005; *Van der Woerd et al.*, 1998, 2000, 2002b]. Finally, we compare these collective results of geologic slip rates against geodetic measures of present-day velocity to assess the potential role of transient deformation associated with the seismic cycle [e.g., *Chevalier et al.*, 2005b; *Mériaux et al.*, 2004]. Together, these measures of fault slip allow us to characterize the deformation field associated with the eastern tip of

the Kunlun fault and to test whether or not slip is transmitted beyond the margin of the Tibetan Plateau.

2. Geologic Background

[6] The Kunlun fault, in east central Tibet, represents one of the key structural elements in the active deformation field of Eurasia [Avouac and Tapponnier, 1993]. The fault marks the northern boundary of the Tibetan Plateau for nearly ~1500 km along strike, delineating a transition from a continuous, low-relief, high-elevation plateau to the south to a northern domain characterized by active high mountain ranges and intramontane basins (Figure 1). The fault is also coincident with the northern boundary of the Songpan-Garze–Hoh Xil terrane along the Anyemaqen-Kunlun suture [Yin and Harrison, 2000]. The timing of initiation of left-lateral shear along the fault system is uncertain, but has been inferred to be coeval with Miocene extension (circa 15 Ma) in the westernmost (west of 91°E) portions of the fault system [Jolivet et al., 2003]. A dearth of geologic piercing points across this boundary, however, has hampered efforts to estimate total displacement across the fault; some studies rely on an apparent deflection (~85 km) of the Yellow River along the easternmost fault segment [Gaudemer et al., 1989; Van der Woerd et al., 2002b]. As we discuss below, our data do not support this interpretation, and we contend that the finite displacement on the fault remains poorly understood.

[7] Slip rates along the Kunlun fault during the Quaternary, in contrast, are fairly well known [Kidd and Molnar, 1988]. Studies of displaced fluvial and glacial landforms along the central ~600 km of the fault (~94°E to ~100°E) indicate slip rates of 11 ± 2 mm/yr over late Pleistocene to Holocene time [Van der Woerd et al., 1998, 2000, 2002b]. An additional study near ~92°E [Li et al., 2005] also yielded mid-Holocene rates of 10 ± 1.5 mm/yr. Together these studies suggest that fault exhibits nearly uniform slip rates along the central ~800 km of its length. This behavior is consistent with the predictions of block-like deformation [Tapponnier et al., 1986], and thus the Kunlun fault is considered to play a key role in models for extrusion of central Tibet [Li et al., 2005; Van der Woerd et al., 2002b].

[8] The central and western segments of the fault have also hosted a series of large earthquakes in the past century, including the recent 2001 Kokoxilli event (M_s 8.1) [Lin et al., 2002; Van der Woerd et al., 2002a]. Together with the 1997 Manyi (M_w 7.6) [Peltzer et al., 1999], 1937 Dongxi Co ($M \sim 7.5$), and two smaller events [cf. Van der Woerd et al., 2002b], nearly the entire length of the fault west of ~100°E has experienced a historic rupture (Figure 1). In contrast, the eastern segments of the fault appear to have experienced little historic seismicity [Gu et al., 1989; Van der Woerd et al., 2002b]. Recent paleoseismic investigations near the town of Maqu (Figure 2), in fact, reveal that the most recent rupture along this segment of the Kunlun fault appears to have occurred between 1700 and 3700 ka [He et al., 2007].

[9] The question of how displacement is accommodated at the eastern tip of the fault remains uncertain. The fault

can be traced as a continuous series of scarps through the Anyemaqen Shan, a broad region of high topography within the eastern Tibetan Plateau between 99° and 102°E (Figure 2), until it is obscured by sediments in the western part of the Rouergai (Zoige) basin (~102°E, Figure 2). Early suggestions that the Kunlun fault linked with active left-lateral faults in the Qinling Shan [e.g., Peltzer et al., 1985; e.g., Zhang et al., 1995] seem untenable in light of this geometry, as linkage between these systems would require a northward step of nearly 200 km (Figure 2). Van der Woerd et al. [2002a] interpreted the fault to continue northward across a broad dilational jog to link up with active faults in the Bailong Jiang (Figure 2). Alternatively, the fault may continue through the Rouergai basin and link, via the Tazang fault (Figure 2) with active shortening structures in the Min Shan [Chen et al., 1994; Kirby et al., 2000]. Finally, it is possible that the fault simply terminates within the Tibetan Plateau, west of the plateau margin.

3. Slip Rates Along the Eastern Kunlun Fault

[10] We seek to test among these scenarios by reconstructing slip and slip rates at several sites distributed along the easternmost segment of the Kunlun fault (Figure 2). In the eastern Anyemaqen Shan, the fault displaces regionally correlative fluvial terraces developed and subsequently abandoned during incision of the Yellow River (Huang He) and its tributaries. Displacements of terrace risers were determined by surveying using a laser rangefinder (centimeter-scale instrumental precision) at two sites separated by ~40 km along the fault (Figure 2). At the western site (Ken Mu Da, site 1), north flowing tributaries drain high topography south of the Yellow River, whereas at the eastern site (Quor Goth Qu, site 2) a large, south flowing tributary drains highlands north of the fault. Left-lateral displacements of terrace risers at each site (Figure 2) allow us to place bounds on the spatial variation of long-term slip rate along the fault. In addition, we examined a third site along the Tazang fault, east of the Rouergai basin (Figure 2) in order to test the hypothesis that high slip rates are transferred via this fault to the Min Shan.

3.1. Determination of Slip Rates From Fluvial Terrace Risers

[11] The use of fluvial terrace risers in the determination of slip rates along strike slip faults is become common practice [e.g., Allen et al., 1991; Meyer et al., 1996; Mériaux et al., 2004, 2005; e.g., Sieh and Jahns, 1984; Van der Woerd et al., 1998, 2002b; Weldon and Sieh, 1985], although the method is still subject to uncertainties in the interpretation of when the terrace riser began to accumulate slip [Mériaux et al., 2005; Van der Woerd et al., 2002b]. Many have assumed that lateral erosion of the riser occurred continuously during fluvial occupation of the adjacent terrace tread [e.g., Van der Woerd et al., 2002b], and thus displacement does not accumulate until abandonment of the adjacent terrace. In this scenario, the best approximation of the terrace riser “age” is the age of abandonment of the lower, inset terrace. Such conditions are likely met in cases

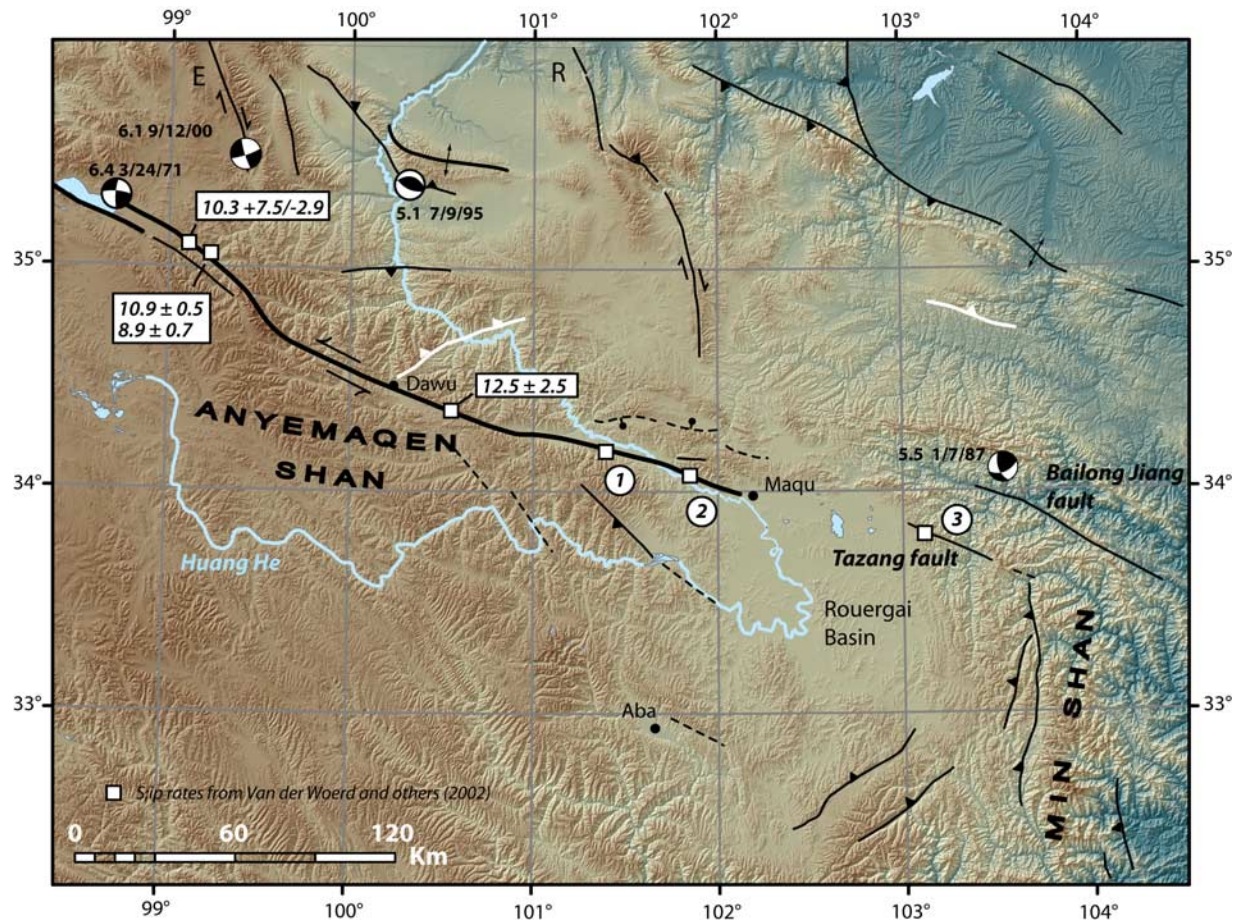


Figure 2. Map of the eastern segment of the Kunlun fault showing location of active faults and major physiographic features. Active faults are represented by heavy lines; dashed where recent activity is inferred. Yellow River (Huang He) is shown as blue line. White boxes represent slip rate estimates (mm/yr) [Van der Woerd et al., 2002b]. Locations of new slip rate determinations are labeled in white circles (1, 2, 3). Focal mechanisms are compiled from USGS (http://neic.usgs.gov/neis/epic/epic_circ.html).

where the channel exhibits limited meandering or braiding and where slip along the fault is such that it displaces terraces into the path of the river. However, when displacement along the fault shields terrace risers from lateral attack, risers may begin to accumulate slip prior to terrace abandonment. In the extreme example, the age of abandonment of the upper terrace may be a more appropriate measure of the average slip rate. The uncertainty imparted by these alternative interpretations of riser age can have a significant impact on the estimate of slip rate [Cowgill, 2007].

[12] It is important to note that in the absence of additional information regarding the history of lateral bank erosion, the first assumption (“lower surface”) provides a maximum bound on the slip rate, whereas the latter view (“upper surface”) yields a minimum bound. Obviously, the ideal sites for slip rates are those with relatively rapid incision, such that the interval between terrace formation and abandonment is short. In this paper, slip rates estimates are presented as both maximum and minimum bounds, utilizing the criteria outlined above, and each

incorporating uncertainties in riser position and radiocarbon chronology.

3.2. Tectonic Geomorphology Along the Eastern Kunlun Fault

[13] Fluvial terraces are ubiquitously developed along tributaries of the Yellow River, west of the town of Maqu (Figure 2), and consist of strath surfaces beveled into indurated and weathered alluvium (of undetermined age). Each terrace bears a thin, 1–2 m tread of fluvial gravel with interbedded sand/silt lenses, and thus they do not appear to record significant aggradation of the fluvial system. Fluvial deposits are overlain by a variably developed soil mantle of aeolian silt (loess) and organic matter. The highest terrace (designated T_5) bears a thick mantle of loess (>4–6 m), whereas inset terraces ($T_4 - T_1$) exhibit significantly thinner loess cover (~1–2 m). We note here that all terrace designations are relative to the number in a given site, increasing from lowest to highest (modern floodplain, T_0). Little to no aeolian material is present on the lowest terraces

Table 1. Radiocarbon Analytical Data^a

Sample	Terrace	Stratigraphic Context	Material	$\delta^{13}\text{C}$, ‰	¹⁴ C Age, ^b years B.P.	Age Range, ^c years B.P.
<i>Site 1: Ken Ma Du</i>						
EK-K-9	T ₄	base of loess	shell	-7.1	13,024 ± 75	15,417 ± 334
EK-K-12	T ₃	fluvial gravel	wood	-16.3	10,660 ± 120	12,560 ± 321
EK-K-13	T ₁	base of loess	charcoal	-22.7	4497 ± 51	5143 ± 168
<i>Site 2: Quor Goth Qu</i>						
EK-K-14a	T ₂	fluvial silt	shell	-7.7	10,527 ± 77	12,476 ± 306
NH-KC-04-H3	T ₂	fluvial silt	shell	-5.6	11,808 ± 66	13,686 ± 167
NH-KC-04-H1	T ₂	fluvial silt	charcoal	-23.1	8661 ± 49	9638 ± 104
NH-KC-04-H2	T ₂	fluvial silt	charcoal	-25.5	9600 ± 1500	11180 ± 3615
NH-KC-04-H4	T ₂	base of loess	charcoal	-24.6	8100 ± 40	9060 ± 60
NH-KC-05-10	T ₁	fluvial sand	shell	-8.2	6343 ± 49	7310 ± 157
NH-KC-05-9	T ₁	fluvial sand	charcoal	-24.8	6345 ± 53	7310 ± 152
NH-KC-05-8	T ₁	base of loess	shell	-9.0	5827 ± 69	6673±173
<i>Site 3: Tazang Fault</i>						
TZ1	T ₁	fluvial silt	charcoal	-26.8	8133 ± 48	9132 ± 131
TZ2	T ₁	soil	peat	-29.0	4168 ± 50	4689 ± 151

^aReported ¹⁴C ages use Libby's half-life (5568 years) and are referenced to the year A.D. 1950.

^bAnalytical uncertainties are reported at 1 σ .

^cCalendar ages calibrated using INTCAL98 [Stuiver *et al.*, 1998]. Associated age range reported at 2 σ .

(T₁ and T₂) and remnant depositional topography remains distinct on these surfaces. In addition, the highest terraces (T₃ and T₄) exhibit incipient pedogenic carbonate accumulation in the B horizon expressed as thin (<1 mm) rinds on the undersides of clasts. Consistency in the degree of pedogenic carbonate development and the extent of loess accumulation between sites suggests that terrace generation and abandonment was broadly correlative between sites. The age of terrace surfaces was determined by dating in situ organic material (primarily charcoal and shell) from alluvial deposits comprising the terrace tread and the lowermost layers of overlying loess/soil deposits (Table 1). Samples were processed and analyzed at the AMS lab at the University of Arizona, and radiocarbon ages were calibrated to calendar years using the CALIB routine of Stuiver and Reimer [Stuiver *et al.*, 1998].

3.2.1. Site 1, Ken Mu Da

[14] The first site is located along a small north flowing tributary of the Yellow River locally known as Ken Mu Da. The tributary is deeply incised (up to 40 m) into moderately indurated alluvium, and five terrace levels are preserved along the valley walls (Figure 3). The highest of these (T₅) is preserved along the west bank of the river and is mantled with a moderately dissected layer of thick loess (up to 6 m). The T₄ terrace is extensively preserved along both sides of the valley as a broad remnant floodplain (Figure 3) and is overlain by a 1–2 m mantle of loess; thin carbonate rinds

are present on clasts in the upper 30 cm of fluvial deposits. Inset below this surface are three, narrow terraces that are preserved only along the eastern valley wall. These terraces all bear thin (<1 m) soils devoid of significant loess that are developed upon 1–2 m treads of fluvial gravel.

[15] The Kunlun fault at this site is characterized by a single fault trace, which bifurcates into two scarps east of the valley (Figure 3), and progressively displaces the three principal terrace risers along the east bank of the Ken Mu Da river in a left-lateral sense. There appears to be a minor extensional component at this site, marked by an apparent vertical separation of the T₂ tread across the fault (Figure 3). The degree of separation (~3 m) is small relative to the lateral displacement, and we focus on the lateral component of fault displacement. The uppermost riser (T₄/T₃) is displaced by 62 ± 3 m; the second riser (T₃/T₂) is displaced by 52 ± 3 m, and the third riser (T₂/T₁) by 31 ± 5 m. The somewhat larger uncertainty on the latter estimate arises from a modern gully developed along the fault trace that has partially eroded the terrace riser, and the subsequent projection errors are greater.

[16] We collected radiocarbon samples from three of the terrace deposits (Figure 3 and Table 1). All samples were collected at the interface between the fluvial deposits and the overlying soil (either at the base of the loess/soil or at the top of the gravel, Table 1) and are thus interpreted to closely approximate the timing of abandonment of the

Figure 3. Slip rate determination at site 1. (a) CORONA photograph showing locations of displaced terraces along the Ken Mu Da river. Fault trace is marked by arrows. (b) Map of displaced terrace risers along the eastern bank of the Ken Mu Da river. The T₄/T₃, T₃/T₂, and T₂/T₁ risers are displaced by 63 ± 3 m (circle a), 52 ± 3 m (circle b), and 31 ± 5 m (circle c), respectively. White circles show approximate locations of radiocarbon samples. (c) Schematic cross section of terrace geometry and relative position in the valley. Circles show the location of radiocarbon samples; corresponding calibrated ages are shown as years before present (see Table 1). (d) Field photograph and stratigraphic relationship of sample EK-K-12, collected at the base of the soil atop the T₃ terrace and interpreted to bound the timing of abandonment of the terrace tread.

terrace. Although the upper 0.5 m of the soil profile atop the T_4 surface is massive and bioturbated, incipient horizonation in the lower 1.5 m of loess suggest little mixing, and we consider it unlikely that samples have been incorporated from higher in the profile. Terrestrial snail shells collected

from the basal 5 cm of loess overlying fluvial deposits atop T_4 thus suggest that abandonment of the broad T_4 floodplain occurred prior to circa 15.5 ka (Table 1). Subsequent incision appears to have been fairly rapid; partially carbonized wood from the gravel-soil interface atop the T_3 terrace

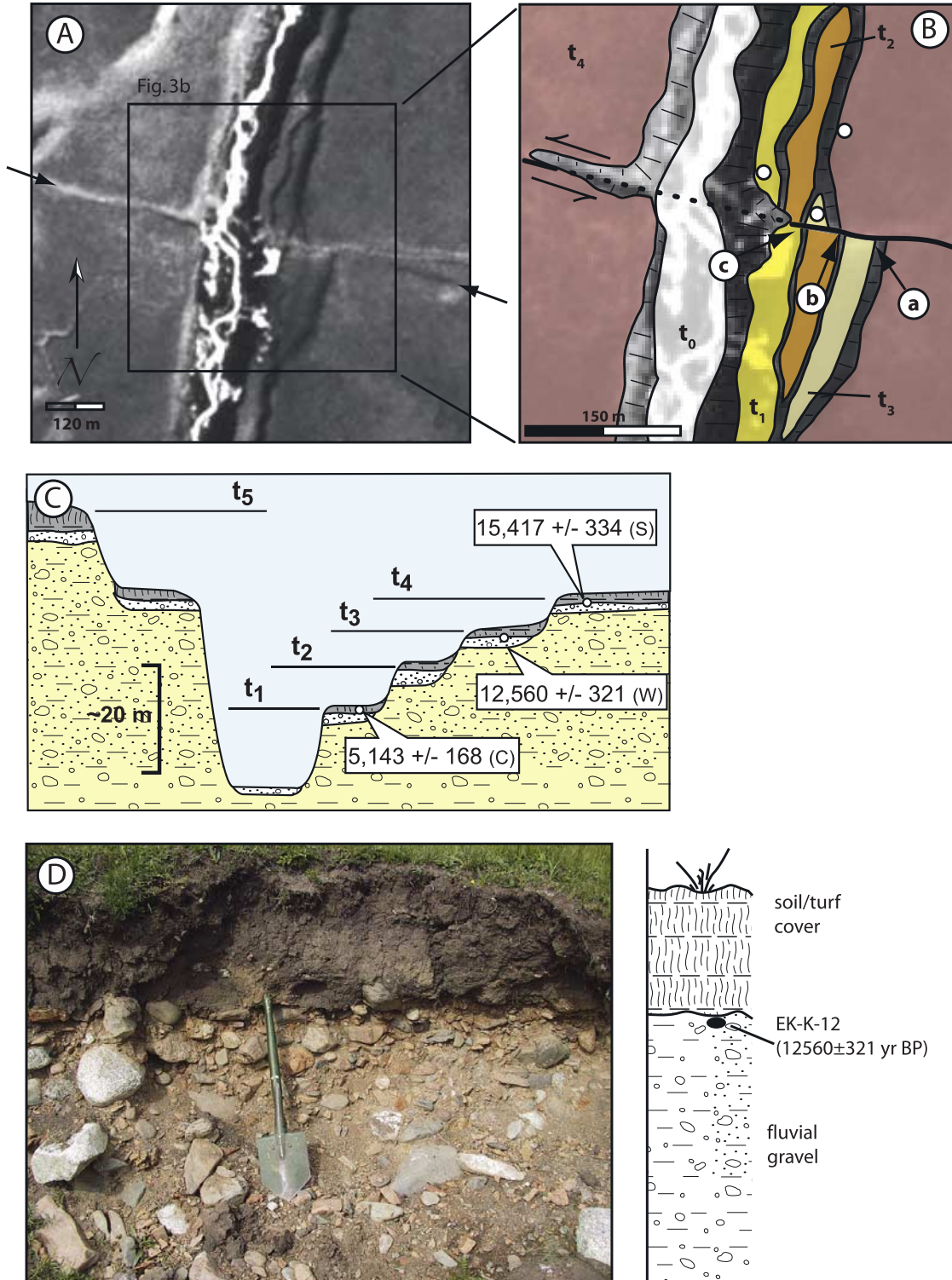


Figure 3

Table 2. Slip Rate Determinations

Riser	Offset, m	Upper Surface	Lower Surface	Maximum Rate, ^a mm/yr	Minimum Rate, ^b mm/yr
<i>Site 1 (Ken Ma Du): 34.20518°N, 101.38593°E</i>					
T ₄ /T ₃	63 ± 3	15,417 ± 334	12,560 ± 321	5.0 ± 0.4	4.1 ± 0.3
T ₃ /T ₂	52 ± 3	12,560 ± 321			4.1 ± 0.4
T ₂ /T ₁	31 ± 5		5,143 ± 168	6.0 ± 1.2	
<i>Site 2 (Quor Goth Qu): 34.11238°N, 101.76128°E</i>					
T ₃ /T ₂	18 ± 4		9,060 ± 60	2.0 ± 0.4	
<i>Site 3 (Tazang Fault): 33.81795°N, 103.10247°E</i>					
T ₁ /T ₀	0	9132 ± 131		<1 ^c	

^aMaximum rate inferred from age of lower (inset) terrace.

^bMinimum rate inferred from age of upper terrace.

^cBound on rate inferred from maximum likely slip event (10 m) and timing of previous rupture.

yielded an age of circa 12.5 ka (Table 1). Finally, charcoal from the basal 5 cm of soil capping the lowest terrace (T₁) yielded an age of circa 5 ka (Table 1), indicating abandonment prior to that time.

[17] As noted above, estimation of the average slip rate over these time intervals depends on when the terrace riser began to accumulate displacement. Fortunately, ages from the T₄ and T₃ terraces provide a fairly narrow interval that brackets the riser age to between circa 15.5 ka and 12.5 ka. Combining these ages with the displacement of the riser (63 ± 3 m) yields a minimum slip rate of 4.1 ± 0.3 mm/yr, using the upper surface age, and a maximum slip rate of 5.0 ± 0.4 mm/yr, using the lower surface age (Table 2). A second bound on the maximum allowable slip rate at this site is provided by utilizing the abandonment age of T₁ (circa 5 ka) and the offset of the T₂/T₁ riser (31 ± 5 m); this relationship indicates slip rates of no greater than 6.0 ± 1.2 mm/yr (Table 2), within uncertainty of the previous estimate. Finally, the age of the T₃ terrace and the displacement of the T₃/T₂ (52 ± 3 m) riser places an additional constraint on the minimum allowable slip rate of 4.1 ± 0.4 mm/yr, nearly identical to the previous estimate.

[18] The close correspondence between both maximum and minimum allowable slip rates from two different terrace risers lends confidence that these estimates represent reliable slip rate determinations. Although we recognize that detrital charcoal incorporated into fluvial deposits can yield erroneously old ages, the fact that our samples all lie either at the interface between the soil and underlying fluvial deposits or within the lower few centimeters of the soil itself argues that these samples were deposited shortly after fluvial deposition on the terrace ceased. Thus the ages are more likely to represent a minimum bound on the timing of terrace abandonment, and our slip rate determinations are likely a maximum estimate.

[19] Moreover, the geomorphology of the site itself suggests that the lower surface model is a more appropriate approximation for the time at which risers began to accumulate displacement. The channel is deeply incised and straight, and all three inset terraces are preserved along the eastern valley wall. Thus we infer that rapid incision of the channel (average rates of ~2 mm/yr) occurred without significant meandering and widening of the floodplain. In

addition, left-lateral displacement of terrace risers preserved along the right bank of the valley (in a reference frame facing downstream) make the downstream risers susceptible to lateral bank erosion by the channel (Figure 3). Both conditions suggest that the assumption that displacement did not begin to accumulate until after abandonment of the inset (lower) terrace is likely met at this site, and we favor the maximum allowable slip rate (5 ± 1 mm/yr) as the best estimate of the slip rate along this portion of the Kunlun fault.

3.2.2. Site 2, Quor Goth Qu

[20] We determined slip rates at a second site, approximately 40 km farther east of Ken Mu Da and 30 km west of the town of Maqu (Figure 2). This site is located north of the Yellow River, and the Quor Goth Qu tributary drains toward the south (Figure 2). Incision along the Yellow River decreases notably from west to east between the two sites, and consequently the tributary at Quor Goth Qu has incised by only ~15 m into the older alluvium. Four terrace levels are preserved along the valley; the highest of these (T₄) is a relict hill of alluvium exposed near the mountain front (Figure 4). Below this level is a broad alluvial fan/terrace complex (T₃) that bears a 1–2 m thick mantle of loessial soil. Fluvial gravels immediately below the loess exhibit thin carbonate collars in the B horizon, similar to those observed in the T₄ terrace at Ken Mu Da. Inset below the T₃ piedmont are two relatively narrow terrace levels. The higher of these (T₂) forms an extensively preserved surface exposed along the entire length of the tributary (Figure 4). Fluvial deposits consist primarily of gravel and minor sand lenses; these are covered by a 50 cm thick loessial soil (Figure 4). The lowest terrace (T₁) forms a discontinuous surface inset 3–5 m below T₂ and is exposed primarily in the lower reaches of the channel, near the Yellow River. The T₁ terrace exhibits a thin 30–50 cm loessial soil (Figure 4).

[21] The Kunlun fault west of the Ken Mu Da drainage is marked by a series of extensional steps that form local sag ponds (Figure 4). These coalesce to form a single scarp that displaces the T₃/T₂ riser along the east side of the valley in a left-lateral sense (Figure 4). There appears to be a minor extensional component at this site, based on a ~2 m apparent vertical separation of the terrace tread (Figure 4). Surveys of the lateral displacement by with laser range-finder and tape indicate that the T₂/T₃ riser is laterally offset

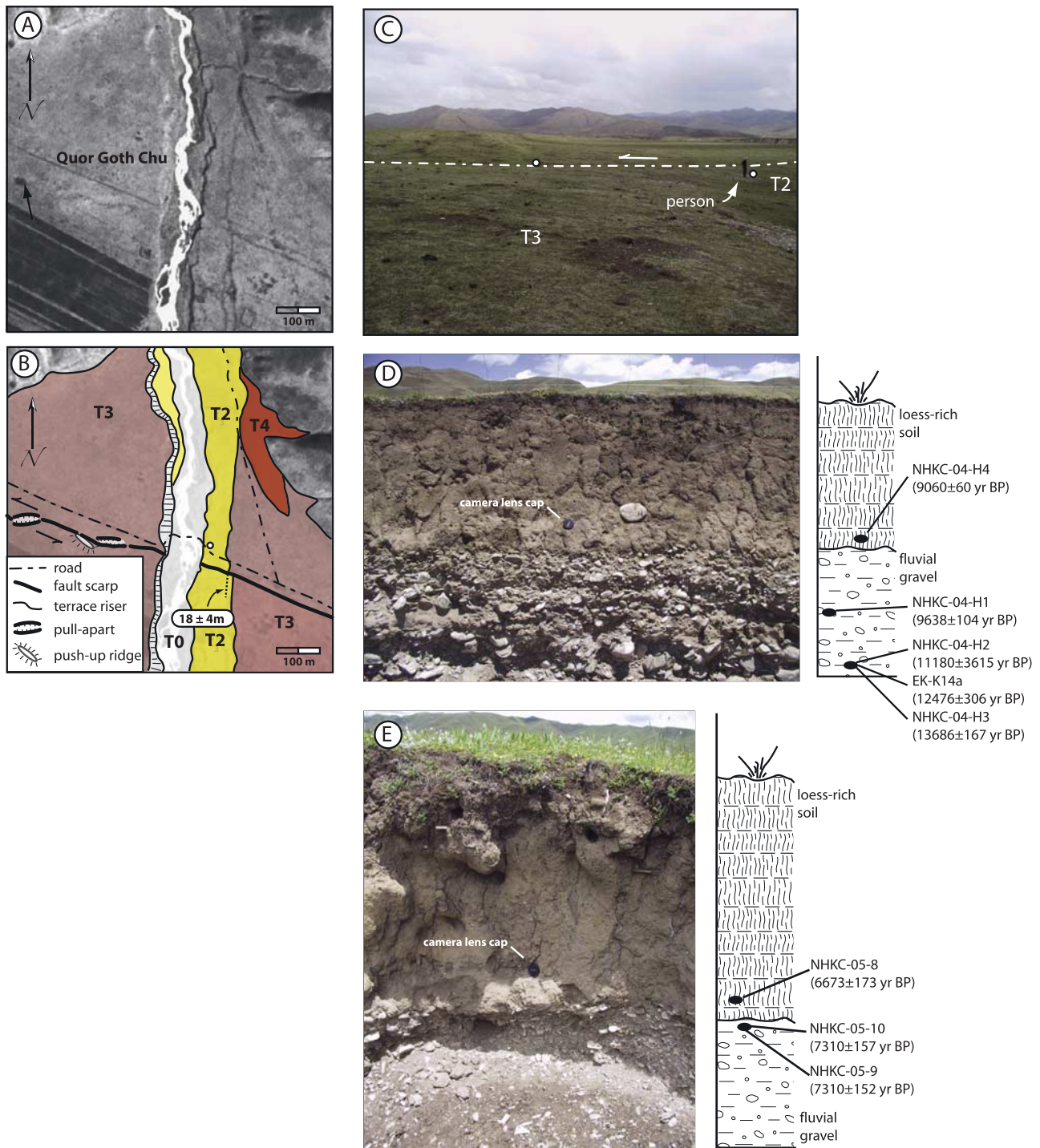


Figure 4. Slip rate determination at site 2. (a) CORONA photograph and (b) geologic map of Site 2 along the Quor Goth Qu river. (c) Photograph looking south along the projection of the T₃/T₂ riser which is displaced left-laterally by 18 ± 4 m. White circles represent the intersection of the base of the riser with the fault trace. (d) Photograph of deposits atop the T₂ terrace. The distribution of ages suggests terrace abandonment between ~ 9.6 and ~ 9.0 ka. (e) Photograph of deposits atop the T₁ terrace, ~ 1 km south of the site above. Ages from fluvial deposits and the overlying loess suggest terrace abandonment between ~ 7.3 and 6.7 ka.

by 18 ± 4 m (Figure 4). The uncertainty arises primarily because of a slight curvature in the riser near the trace of the fault (Figure 4).

[22] We collected radiocarbon samples from both fluvial deposits and overlying loess on the T_2 and T_1 terrace levels. Both shell material and charcoal from silt and sandy lenses in T_2 gravels yield a range of ages between circa 9.6 ka and 13.6 ka (Table 1). The wide range of ages may reflect (1) long-lived occupation of the terrace surface, consistent with the relatively limited incision at this site and/or (2) incorporation of older organic material into the fluvial deposits. Regardless, a sample of charcoal from the lower 5 cm of the overlying loess on T_2 indicates abandonment of this surface was locally accomplished by circa 9 ka (Table 1). This is consistent with samples from the inset T_1 terrace; two samples of shell and charcoal from a silt lens within terrace deposits yielded identical ages of circa 7.3 ka, and a sample of shell material from the basal portion of the overlying loess yielded a younger age of circa 6.7 ka (Table 1).

[23] Combining the timing of abandonment of the T_2 terrace surface with the observed offset of the T_3/T_2 terrace riser (18 ± 4 m) yields an average slip rate of 2.0 ± 0.4 mm/yr (Table 2). This rate represents a maximum estimate as it assumes that the riser offset accumulated entirely after abandonment of the T_2 surface. We note that the relatively low incision rates and apparent long-lived occupation of the T_2 surface are favorable conditions for lateral erosion by the channel, and thus we interpret this rate estimate as a reasonable value for this portion of the fault. If any slip accumulated prior to T_2 abandonment, however, the actual slip rate could be somewhat lower.

3.2.3. Constraints on Slip Along the Tazang Fault

[24] East of the town of Maqu, the trace of the Kunlun fault is obscured within the marshlands of the Rouergai basin, but projects directly along strike toward the Tazang fault (Figure 2). The fault appears as a sharp trace on satellite images (Figure 5) and displaces bedrock interfluves in an apparent left-lateral sense. This structure extends for ~ 50 km toward the east appears to link with the Min Jiang fault system (Figure 2) in the remote, high-relief valleys in the headwaters of the Bailong Jiang (White Dragon River). Thus the Tazang fault is one of the primary candidates to transfer slip from the Kunlun fault to shortening structures at the margin of the Tibetan Plateau [Chen *et al.*, 1994; Kirby *et al.*, 2000; Van der Woerd *et al.*, 2002b]; we consider the other, the Bailong Jiang fault, in section 5.1.

[25] We examined sites along the western 20 km of the fault, near its intersection with the Rouergai Basin. Immediately east of the basin, three small catchments are deflected in a left-lateral sense across the fault (Figure 5). On the interfluves, the fault forms a uphill-facing scarp that separates low bedrock hills on the south from a higher relief range to the north (Figure 5). Broad aggradational fill terraces are developed in all three of the watersheds, but none of these exhibit any topographic disruption where they cross the fault (Figure 5). Moreover, incision into the alluvial fill has generated steep cut banks along the channel walls that cross the projection of the fault and act as natural trench exposures 6–8 m deep (Figure 5). The terrace fill is

composed of a lower 3–4 m of fine-grained alluvial silt and sand; bedding is relatively planar. This unit is buried beneath a 3–4 m thick soil composed primarily of turf and peat (Figure 5). Stratigraphy within stream banks is continuous across the fault (Figure 5); we observed no evidence of recent faulting within the terrace fill in three catchments. Thus we conclude that the most recent rupture along the Tazang fault predates the aggradation event that generated the terrace fill.

[26] We obtained two charcoal samples from the terrace fill to constrain the timing of aggradation. A sample of charcoal from an organic-rich silt lens in the lower fluvial unit, approximately 2 m above the channel floor (Figure 5), yielded a calibrated age of 9132 ± 131 years B.P., and a peat layer from the overlying soil, approximately 1.5 m above the fluvial unit, yielded an age of 4689 ± 151 years B.P. (Table 1). These ages suggest moderate aggradation (~ 1 mm/yr) between 9 and 4 ka, and subsequently rapid incision in the late Holocene. More importantly, the fact that terrace deposits are not displaced by the Tazang fault suggests that the last rupture occurred sometime prior to circa 9 ka.

[27] Although geologic relationships along the Tazang fault do not allow us to estimate an average slip rate, we can place some broad constraints from consideration of typical rupture magnitudes. If the Tazang fault ruptures infrequently, but large events characteristic of major strike systems (6–9 m slip per event for $M \sim 8$ [e.g., Wells and Coppersmith, 1994]), the single-event slip rate would still be < 1 mm/yr. Of course, if seismic strain release was temporally clustered, the allowable rate could be somewhat greater, but without detailed paleoseismic records to support such conjecture, we consider it likely Tazang fault is moving slowly, at rates less than ~ 1 mm/yr. The Tazang fault appears to link eastward with the north striking Min Jiang fault system [Chen *et al.*, 1994], and we note that a low slip rate along the Tazang fault is consistent with the relatively low rates of shortening inferred for the Min Jiang fault system (~ 1 mm/yr) over late Pleistocene–Holocene time [Kirby *et al.*, 2000].

3.3. Summary of Geologic Slip Rates

[28] Taken together, our data reveal a progressive decrease in the rate of slip along the eastern Kunlun fault over late Pleistocene–Holocene time, from > 10 mm/yr along the central portion of the fault [Van der Woerd *et al.*, 2002b], to < 6 mm/yr at site 1 (Ken Mu Da), to ~ 2 mm/yr at site 2 (Quor Goth Qu). It is important to note that the magnitudes of the observed displacements (> 20 m in all cases) require accumulation during multiple seismic events, and thus the decrease in rate probably does not reflect an artifact of averaging over a time period with anomalously low seismicity. Our results further suggest that slip rates along the Tazang fault are quite low (≤ 1 mm/yr), and it appears unlikely that this fault system transfers a significant portion of slip to shortening in the Min Shan region.

4. Correspondence With Geodetic Velocities

[29] Among the insights gained by the advent of high-precision space geodesy (GPS) is a growing recognition that

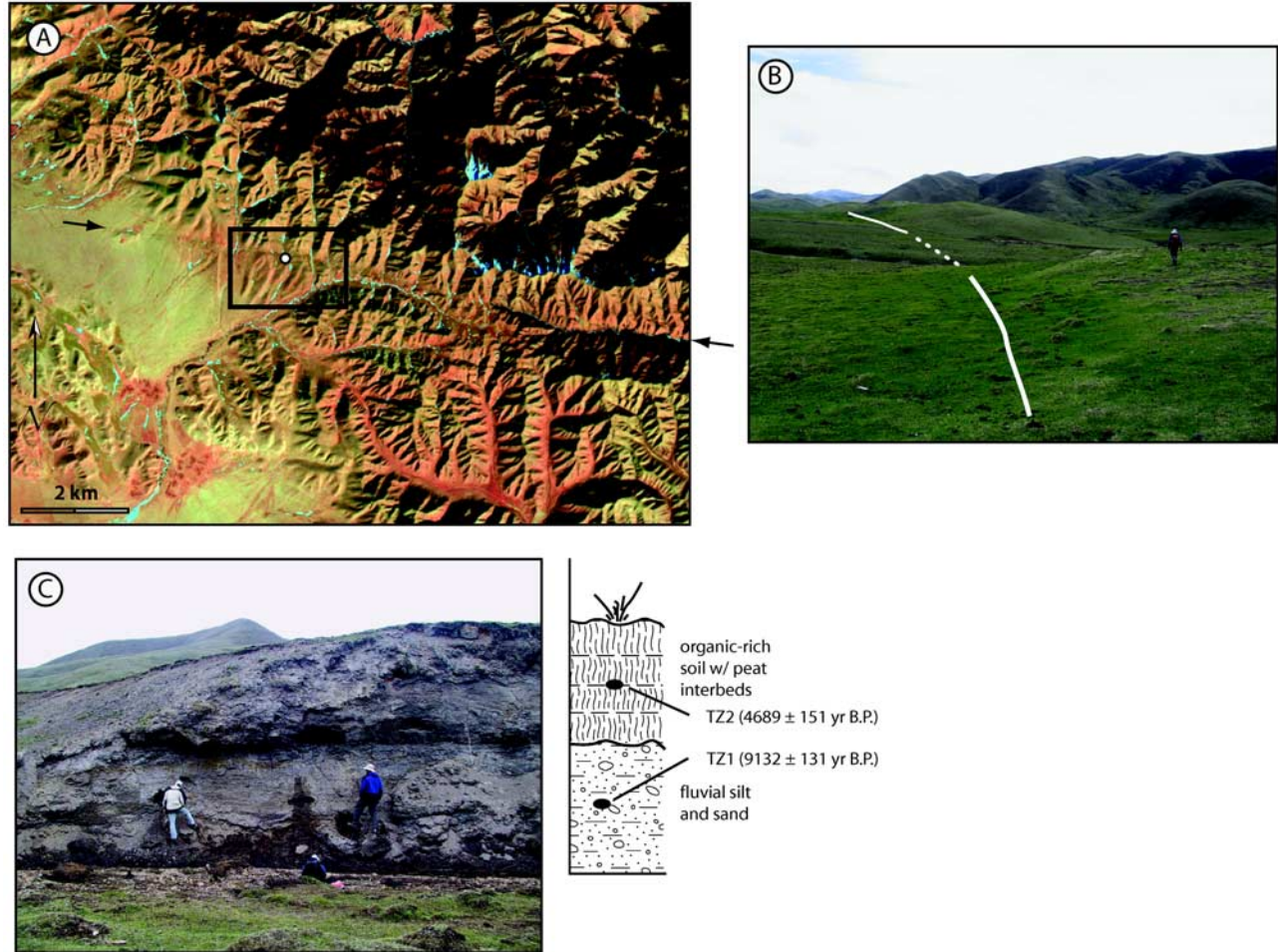


Figure 5. Bounds on slip rate along the Tazang fault at site 3. (a) LANDSAT TM image (bands 7, 4, 1) of the Tazang fault, visible as a sharp trace (arrows) that deflects drainages in a left-lateral sense (box). White circle shows location of photographs in Figures 5b and 5c. (b) Photograph looking west along the surface trace of the Tazang fault. Scarp faces north (uphill) and restricts drainage from the watersheds north of the fault. Scarp does not disrupt fill terrace surface in midground. (c) Cut-bank exposure of terrace fill along projected trace of Tazang fault. Strata are continuous and apparently undisturbed. Radiocarbon samples from fluvial silt and from overlying peat-rich soil indicate that the fault has not ruptured in the past ~ 9 kyr.

a number of intracontinental fault systems exhibit differences between long-term (geologic) slip rates and those inferred from short-term (decadal) measurements of surface velocity [Bendick *et al.*, 2000; Meyer *et al.*, 1996; Mériaux *et al.*, 2004, 2005; Wright *et al.*, 2004]. Although such differences may reflect transient behavior associated with the seismic cycle [e.g., Chevalier *et al.*, 2005b] or with fault system evolution [e.g., Bennett *et al.*, 2004], the significance of such differences remains contentious due to contrasting interpretations of geologic data [cf. Brown *et al.*, 2005; Chevalier *et al.*, 2005a]. In this section, we utilize published geodetic velocity fields for central and eastern Tibet [Shen *et al.*, 2005; Zhang *et al.*, 2004] to examine the degree of correspondence between geologic slip rates and geodetic velocities along the length of the Kunlun fault and to test whether strain may be accumulating at the tip of the fault.

[30] Although existing data are sparse along much of the Kunlun fault (Figure 6), a NE–SW transect along the Lhasa–Golmud road crosses the fault near 94°E . Velocities resolved parallel to fault strike permit slip rates between 8 and 12 mm/yr, consistent with geologic rates along this portion of the fault [Van der Woerd *et al.*, 1998, 2002b]. We illustrate this with a simple elastic dislocation model [e.g., Savage and Burford, 1973] in Figure 6b, although a more sophisticated attempt at inverting the surface velocity field along this transect for parameters describing a viscoelastic rheology of the crust yields fundamentally the same result (optimal slip rate of ~ 10 mm/yr [Hilley *et al.*, 2005]). Thus along the central Kunlun fault, there does not appear to be a significant difference in the rate inferred over geologic or decadal time intervals.

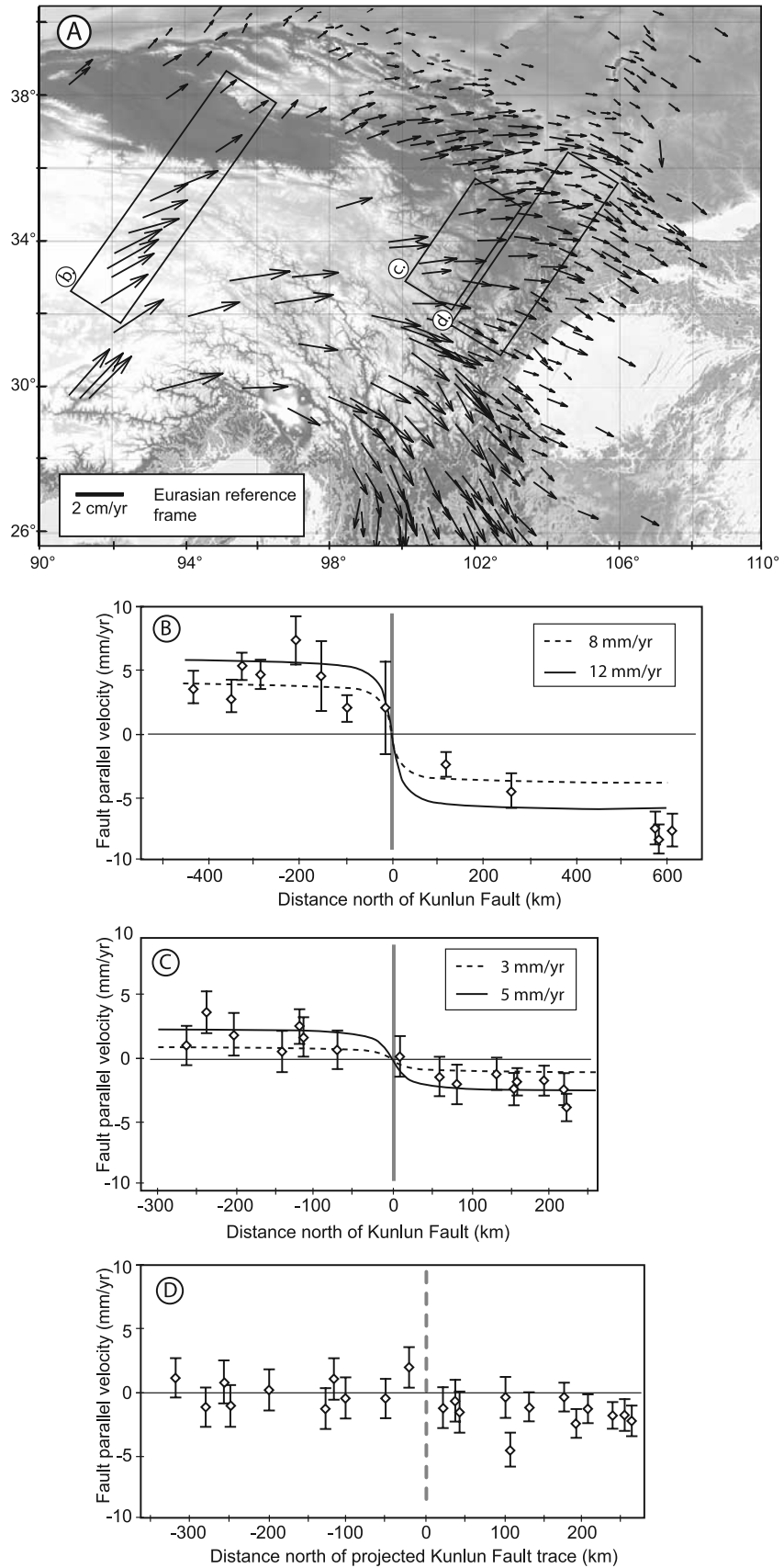


Figure 6

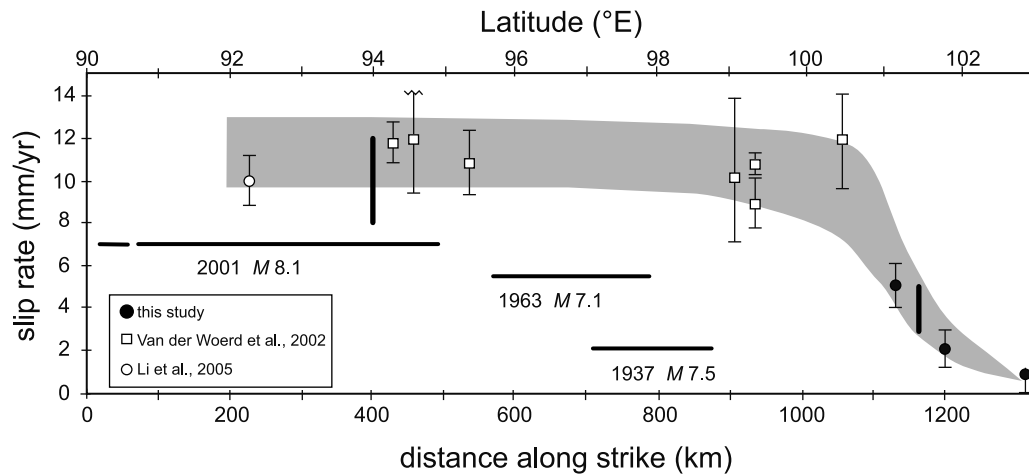


Figure 7. Compilation of slip rate estimates and recent seismicity along the Kunlun fault. Open and shaded boxes represent slip rate estimates from previous studies, dark circles new slip rates presented in this work, and heavy vertical lines represent the allowable range of slip rates from geodetic velocities. The lateral extent of previous ruptures along the Kunlun fault are depicted for earthquakes in 1937 [Li et al., 2005; Tapponnier and Molnar, 1977] and 1963 [Tapponnier and Molnar, 1977] and for the 2001 Kokoxili event [Lin et al., 2002; Van der Woerd et al., 2002a]. Note that slip rates (gray shading) decrease markedly toward the eastern tip of the fault, coincident with an absence of historic seismicity and imply strain accumulation in the surrounding Tibetan Plateau.

[31] In contrast, fault-parallel velocities along a second transect at the eastern end of the Kunlun fault (centered at approximately 101.5°E, Figure 6) suggest slip rates of no greater than 3–5 mm/yr (Figure 6c). This location of this transect is nearly coincident with site 1 (Ken Mu Da), and these slip rates are similar to those inferred from our geologic data. Finally, a third transect located farther east (centered at approximately 102.5°E) intersects the projection of the Kunlun fault along the Tazang fault. Fault-parallel velocities are permissible of perhaps 1–2 mm/yr of left-lateral shear but are within uncertainty of zero (Figure 6d).

[32] In summary, available geodetic data agree well with geologic slip rates both along the central portion of the fault and at the eastern tip. Notably, over both intervals of time, slip rates decrease systematically from west to east over the eastern ~100–150 km of the fault system. The relatively long interval since the last rupture along the eastern segments of the fault system (i.e., >1.8 kyr near Maqu [He et al., 2007] and >9 kyr along the Tazang fault) suggests that the fault is late in the seismic cycle, and geodetic velocities should therefore closely approximate the far-field elastic loading rate [e.g., Malservisi et al., 2003]. The correspondence between the interseismic velocity field and our determinations of late Pleistocene–Holocene

slip rate suggest that both measures of fault slip reveal gradients in displacement and displacement rate near the eastern fault tip.

5. Discussion

[33] Our results suggest that the easternmost segment of the Kunlun fault exhibits slip rates that are a factor of 2 to 6 lower than rates determined for the central ~600–800 km of the fault [e.g., Li et al., 2005; e.g., Van der Woerd et al., 2002b]. Moreover, slip rates appear to decrease systematically with position along the fault (Figure 7). These results challenge the idea that slip rates remain uniform along the entire length of the Kunlun fault [Van der Woerd et al., 2002b], but rather seem to indicate that slip dies out along strike. Both studies utilize late Pleistocene–Holocene geomorphic markers of displacement, and thus it is unlikely that the difference between them simply reflects incomplete averaging of the seismic cycle. Moreover, our results match geodetic velocities that resolve little left-lateral shear across the eastern Kunlun fault [Chen et al., 2000; Shen et al., 2005; Zhang et al., 2004]. These three of these studies rely on independent surveys of different control points, thus providing a measure of confidence that the absence of

Figure 6. Geodetic velocities across the Kunlun fault. (a) Map of velocity vectors relative to a stable Eurasian reference frame. Data compiled from Shen et al. [2005] and Zhang et al. [2004]. (b–d) Fault-parallel velocities (110° azimuth) in transects located across the central portion of the fault (Figure 6b), the eastern fault tip (Figure 6c), and the Tazang fault (Figure 6d). Solid lines represent velocities predicted from a dislocation model in an elastic half-space with a locking depth of 15 km and serve to illustrate the range of reasonable slip rates permitted by the data. Position of Kunlun fault shown as vertical line.

velocity gradients across this region of the plateau is real. Therefore we argue that our results reveal spatial gradients in slip rate along the eastern Kunlun fault (Figure 7) that appear to be a relatively long-lived feature of this fault system. In what follows, we explore hypotheses for mechanisms by which displacement gradients may be accommodated at the eastern tip of the Kunlun fault.

5.1. Transfer to the Bailong Jiang Fault System

[34] One of the principal hypotheses for the termination of the Kunlun fault system is that displacement is transferred via the Bailong Jiang and Tazang fault systems (Figure 2) to shortening structures adjacent to and north of the Sichuan Basin [Chen *et al.*, 1994; Kirby *et al.*, 2000; Van der Woerd *et al.*, 2002b]. Our work indicates that most direct of these proposed linkages, to the Tazang fault, appears to accommodate little, if any, of the displacement along the eastern Kunlun fault. Here we address the alternate hypothesis that slip is accommodated along the Bailong Jiang fault zone.

[35] We consider it unlikely that the Bailong Jiang fault accommodates a significant component of slip from the Kunlun fault for several reasons. First, although the Bailong Jiang fault appears to be active, in that it displaces bedrock interfluves, the western extent of this activity can only be traced into the headwaters of the Bailong Jiang (Figure 2). There are no active faults recognizable in the field or on remote sensing between the eastern tip of the Kunlun fault near Maqu (Figure 2) and the western end of the Bailong Jiang fault, a distance of over 100 km. Second, such a geometry would predict a significant extensional component, for which there is no evidence. In fact, the intervening ranges between the eastern end of the Kunlun and the Bailong Jiang faults comprise relatively high, rugged topography. In contrast, a releasing step in the fault system occurs at Dongxi Co, just west of 99°E (Figure 2), and in this location the geometry is responsible for the development of an extensional basin [Van der Woerd *et al.*, 2002b]. Finally, ongoing work along the Bailong Jiang fault by researchers from the Institute of Geology, China Earthquake Administration in Gansu suggests that the fault is characterized by relatively low slip rates (<3 mm/yr (Yuan Daoyang, personal communication, 2006)).

5.2. Similarity to Displacement Gradients Along Crustal Faults

[36] The fact that slip along the Kunlun fault does not appear to link with structures at the margin of the Tibetan Plateau indicates that displacement must somehow be absorbed by deformation in the volume surrounding the fault tip. Such behavior is directly analogous to that inferred from scaling relationships between fault displacement and length [e.g., Cowie and Scholz, 1992a; Stirling *et al.*, 1996]. Linear displacement gradients typically observed near fault tips ($x/L \geq 0.75$, where x is the position along the fault and L is the fault half length) are suggested to reflect a finite yielding in a damage zone surrounding the fault tip [Cowie and Scholz, 1992a, 1992b; Cowie and Shipton, 1998]. Existing data for strike-slip faults are consistent with this

model [Peacock, 1991]. Few data are available, however, for intracontinental faults of the scale of the Kunlun [Stirling *et al.*, 1996]. Theoretical treatment of a fault tip embedded in a viscous medium predicts that displacement gradients should depend on the average rheology of the crust [Barr and Houseman, 1992, 1996]. Our data are not yet sufficient to distinguish whether displacement gradients on the Kunlun fault decrease linearly toward the fault tip [e.g., Peacock, 1991] or in some other way. This will be discussed in greater detail in a forthcoming paper. However, despite their preliminary nature, our results indicate that the Kunlun fault does not behave as a simple transfer structure. Rather, it appears that the termination of the fault system requires deformation of the regions of the plateau surrounding the fault tip (cf. Zhang *et al.*, submitted manuscript, 2006).

5.3. Mechanisms to Accommodate Displacement Gradients

[37] The question of how displacement gradients are accommodated by deformation within the plateau, however, remains uncertain. In this section, we explore three hypotheses that are compatible with our observations of slip rate gradients along the eastern Kunlun fault. None of these are mutually exclusive, and it is possible that components of each are operating in eastern Tibet. Nonetheless, we pose them as a means to further future work on the question.

5.3.1. Eastward Propagation of the Kunlun Fault

[38] The presence of displacement gradients near the tip of the Kunlun fault suggests that the fault may simply be relatively immature and that the system has not yet accumulated significant finite displacement. If so, the fault may be growing in length, and the tip may be propagating toward the east in a manner similar to that suggested for crustal fault systems [e.g., Cowie and Scholz, 1992b; Dawers *et al.*, 1993] as well as for the North Anatolian fault [Flerit *et al.*, 2004]. Two lines of evidence, however, argue against this scenario. First, we do not observe high geodetic velocities near the fault tip, as might be expected if strain was accumulating in response to gradients in displacement. Rather, the geodetic velocities appear to decrease toward the east over length scales of $\sim 10^3$ km (Figure 6), similar to those inferred from geologic slip rates. In addition, the apparently long interseismic intervals inferred for the eastern Kunlun fault [He *et al.*, 2007] are consistent with slow strain accumulation. Unfortunately, the lack of markers with which to track finite displacement over longer time intervals than our study prevents a definitive test of this hypothesis at present, and it remains possible that the fault is growing eastward with time.

5.3.2. Crustal Thickening in the Anyemaqen Shan

[39] The Anyemaqen Shan are a broad, elliptical region of high topography surrounding the eastern ~ 300 km of the Kunlun fault (Figure 2) that marks a step from elevations of ~ 4500 m on the plateau to the southwest to somewhat lower elevations (~ 3500 m) on the plateau north and east of the range (Figure 2). The association between high relief within the range and the tip of the fault suggest the possibility that active crustal thickening in the Anyemaqen

absorbs some component of the displacement along the Kunlun fault. Several minor active faults in the southeastern part of the range (Figure 2) exhibit an apparent shortening component, consistent with distributed shortening around the fault tip. In addition, we observed a thrust sense separation of an alluvial fan surface along a minor fault in the northern Anyemaqen (Figure 2). Although the slip rates along these structures are uncertain, they appear to indicate at least some degree of active deformation within the range. We also note that recent work on the geomorphology of the range suggests that there are systematic spatial patterns in erosion rate that may reflect active differential rock uplift across the range (N. Harkins et al., Transient fluvial incision in the headwaters of the Yellow River, northeastern Tibetan Plateau, China, submitted to *Journal of Geophysical Research*, 2006). A quantitative analysis of the relationship of this deformation to the fault tip is, however, beyond the scope of this paper.

5.3.3. Rotation of the Kunlun Fault

[40] As pointed out by *England and Molnar* [1990], the cognitive leap from the observation of rapid displacement along strike-slip faults to the interpretation of eastward extrusion of Asian lithosphere carries the implicit assumption that the faults themselves are fixed, and do not rotate. Geologic and geodetic evidence from eastern and southeastern Tibet, however, indicates that the deformation field has been characterized by significant clockwise rotation of material around the eastern syntaxis of the Himalaya [*Burchfiel*, 2004; *Chen et al.*, 2000; *Holt et al.*, 1991; *King et al.*, 1997; *Molnar and Lyon-Caen*, 1989; *Shen et al.*, 2005]. Similar velocity gradients in northeastern Tibet define a broad (>300 km wide) NE trending zone of right-lateral shear that coincides with the eastern tip of the Kunlun fault (Figure 2) [*Shen et al.*, 2005]. Rotation of material lines are predicted to be clockwise across this shear zone, and if the Kunlun fault is rotating, then the eastern termination of the fault may merely reflect the eastern extent of this broad shear zone.

[41] Simple models of rigidly rotating blocks imply that displacement should remain constant along the fault, even if the faults are rotating. This has been cited as evidence that rotation of faults with constant curvature will only change the direction of extrusion, not its magnitude [e.g., *Avouac and Tapponnier*, 1993]. It is important to note, however, that if the curvature of the faults is not constant (as in the case of the Kunlun), the bounding regions must deform internally. North of the Kunlun fault, velocity gradients appear to be accommodated by coupled shortening on E–W fault systems and right-lateral displacement along NNW striking faults (Elashan and Riyueshan faults, Figure 1). It is intriguing to note that these faults roughly coincide with the western and eastern extents of the Anyemaqen Shan (Figure 1), and that the Elashan fault coincides with the large restraining bend along the Kunlun fault in the western part of the range (Figure 2). We speculate that the complex geometry of the easternmost segments of the Kunlun fault could be a consequence of rotation of the fault in response to differential amounts of shortening across northeastern Tibet. A definitive test of this hypothesis, however, requires

a significantly more comprehensive understanding of the distribution and timing of both deformation in the region than is presently available.

6. Tectonic Implications

[42] At the heart of the debate over the rates of deformation throughout the Indo-Asian collision lies a fundamental question: Do the rules of plate tectonics govern deformation within continental lithosphere? An obvious yet profound consequence of slip rate gradients along the eastern Kunlun fault is that displacement along the fault is not transmitted beyond the eastern margin of the Tibetan Plateau. In fact, our results imply that slip rates decrease to <2 mm/yr near $\sim 102^\circ\text{E}$ (Figure 7), some 150–200 km west of the plateau margin. Thus to the degree that the Kunlun fault is responsible for extrusion of central and northern Tibet, it must be limited to the confines of the Tibetan Plateau itself. We acknowledge that this conclusion strictly pertains to displacement over the past circa 10–20 ka. However, it seems to us unlikely that the Kunlun fault accommodated large finite displacements at its eastern termination at some time deeper in the geologic past. The magnitude of shortening adjacent to the Sichuan Basin (<10 km [*Burchfiel et al.*, 1995]) and in the Min Shan (<1–10 km [*Kirby et al.*, 2000]) appears to be consistent with limited finite displacement at the tip of the Kunlun fault.

[43] Our results further suggest that the evolution of the eastern Kunlun fault is fundamentally linked to the thickened crust of the plateau. In contrast to the transform-like behavior of the Altyn Tagh and perhaps the Haiyuan fault systems, slip along the Kunlun fault is not absorbed by shortening at the plateau boundary. We infer that the presence of slip rate gradients along the eastern Kunlun fault implies that regions of the plateau surrounding the fault tip must be deforming internally in order to maintain strain compatibility. Thus our results support hypotheses that link lateral displacement with continuum models for plateau deformation [*England and Molnar*, 2005, 1990].

[44] Moreover, even if the fault is propagating toward the east, it does not appear to drive plateau growth in the manner suggested by *Tapponnier et al.* [2001]. Rather, crustal thickening appears to lead, not lag, fault growth. This association suggests that deformation of the upper crust may be decoupled from deformation at depth. We note that there is mounting evidence for a weak lower crust in this part of eastern Tibet [*Clark et al.*, 2005; *Clark and Royden*, 2000; *Royden et al.*, 1997], and we suspect this rheologic condition exerts a profound influence on the distribution of deformation around the fault tip [*Barr and Houseman*, 1996].

[45] Finally, our study demonstrates that rapid and slow displacement may coexist along a single structure and highlights the necessity of studying the manner in which fault displacement and off-fault strain interact. The question of whether displacement rates along Eurasian strike-slip faults are low or high is an important, but not sufficient, test of their geodynamic significance. We expect that further investigation of deformation near the tips of other faults will

reveal similar displacement gradients (e.g., Zhang et al., submitted manuscript, 2006) that will lend further insight into the large-scale mechanics of continental deformation in Eurasia. Despite uniform slip along the central portion of the fault, displacement along the Kunlun fault is not transmitted beyond the eastern margin of the plateau and thus the fault does not accommodate extrusion of central Tibet.

References

- Allen, C. R., Z. Luo, H. Qian, X. Wen, H. Zhou, and W. Huang (1991), Field study of a highly active fault zone: The Xianshuhe fault of southwestern China, *Geol. Soc. Am. Bull.*, *103*, 1178–1199.
- Avouac, J. P., and P. Tapponnier (1993), Kinematic model of active deformation in central Asia, *Geophys. Res. Lett.*, *20*, 895–898.
- Barr, T. D., and G. A. Houseman (1992), Distribution of deformation around a fault in a non-linear ductile medium, *Geophys. Res. Lett.*, *19*, 1145–1148.
- Barr, T. D., and G. A. Houseman (1996), Deformation fields around a fault embedded in a non-linear ductile medium, *Geophys. J. Int.*, *125*, 473–490.
- Bayasgalan, A., J. Jackson, J. Ritz, and S. Carretier (1999), Field examples of strike-slip fault terminations in Mongolia and their tectonic significance, *Tectonics*, *18*, 394–411.
- Bendick, R., R. Bilham, J. Freymueller, K. Larson, and G. Yin (2000), Geodetic evidence for a low slip rate in the Altyn Tagh fault system, *Nature*, *404*, 69–72.
- Bennett, R. A., A. M. Friedrich, and K. P. Furlong (2004), Codependent histories of the San Andreas and San Jacinto fault zones from inversion of fault displacement rates, *Geology*, *32*, 961–964.
- Brown, E. T., R. Bendick, D. L. Bourlès, V. Gaur, P. Molnar, G. M. Raisbeck, and F. You (2002), Slip rates of the Karakorum fault, Ladakh, India, determined using cosmic ray exposure dating of debris flows and moraines, *J. Geophys. Res.*, *107*(B9), 2192, doi:10.1029/2000JB000100.
- Brown, E. T., P. Molnar, and D. L. Bourlès (2005), Comment on “Slip-rate measurements on the Karakorum fault may imply secular variations in fault motion,” *Science*, *309*, 1326b.
- Burchfiel, B. C. (2004), New technology; new geological challenges, *GSA Today*, *14*, 4–10.
- Burchfiel, B. C., et al. (1989), Intracrustal detachments within zones of intracontinental deformation, *Geology*, *17*, 448–452.
- Burchfiel, B. C., Z. Chen, Y. Liu, and L. H. Royden (1995), Tectonics of the Longmen Shan and adjacent regions, *Int. Geol. Rev.*, *37*, 661–735.
- Chen, S. F., C. J. L. Wilson, Q. D. Deng, X. L. Zhao, and Z. L. Luo (1994), Active faulting and block movement associated with large earthquakes in the Min Shan and Longmen Mountains, northeastern Tibetan Plateau, *J. Geophys. Res.*, *99*, 24,025–24,038.
- Chen, Z., B. C. Burchfiel, Y. Liu, R. W. King, L. H. Royden, W. Tang, E. Wang, J. Zhao, and X. Zhang (2000), Global Positioning System measurements from eastern Tibet and their implications for India/Eurasia intercontinental deformation, *J. Geophys. Res.*, *105*, 16,215–16,228.
- Chevalier, M.-L., et al. (2005a), Response to comment on “Slip-rate measurements on the Karakorum fault may imply secular variations in fault motion,” *Science*, *309*, 1326c.
- Chevalier, M.-L., et al. (2005b), Slip-rate measurements on the Karakorum Fault may imply secular variations in fault motion, *Science*, *307*, 411–414.
- Clark, M. K., and L. H. Royden (2000), Topographic ooze: Building the eastern margin of Tibet by lower crustal flow, *Geology*, *28*, 703–706.
- Clark, M. K., J. W. M. Bush, and L. H. Royden (2005), Dynamic topography produced by lower crustal flow against rheologic strength heterogeneities bordering the Tibetan Plateau, *Geophys. J. Int.*, *162*, 575–590.
- Cowgill, E. (2007), Impact of riser reconstructions on estimation of secular variation in rates of strike-slip faulting: Revisiting the Cherchen River site along the Altyn Tagh Fault, NW China, *Earth Planet. Sci. Lett.*, *254*, 239–255.
- Cowie, P. A., and C. H. Scholz (1992a), Displacement-length scaling relationship for faults: Data synthesis and discussion, *J. Struct. Geol.*, *14*, 1149–1156.
- Cowie, P. A., and C. H. Scholz (1992b), Physical explanation for the displacement-length relationship of faults using a post-yield fracture mechanics model, *J. Struct. Geol.*, *14*, 1133–1148.
- Cowie, P. A., and Z. K. Shipton (1998), Fault tip displacement gradients and process zone dimensions, *J. Struct. Geol.*, *20*, 983–997.
- Dawers, N. H., M. H. Anders, and C. H. Scholz (1993), Growth of normal faults: Displacement-length scaling, *Geology*, *21*, 1107–1110.
- England, P., and G. Houseman (1986), Finite strain calculations of continental deformation: 2. Comparison with the India-Asia collision zone, *J. Geophys. Res.*, *91*, 3664–3676.
- England, P. C., and P. Molnar (1990), Right-lateral shear and rotation as the explanation for strike-slip faulting in eastern Tibet, *Nature*, *344*, 140–142.
- England, P., and P. Molnar (2005), Late Quaternary to decadal velocity fields in Asia, *J. Geophys. Res.*, *110*, B12401, doi:10.1029/2004JB003541.
- Flerit, F., R. Armijo, G. King, and B. Meyer (2004), The mechanical interaction between the propagating North Anatolian Fault and the back-arc extension in the Aegean, *Earth Planet. Sci. Lett.*, *224*, 347–362.
- Gaudemer, Y., P. Tapponnier, and D. L. Turcotte (1989), River offsets across active strike-slip faults, *Ann. Tectonicae*, *3*, 55–76.
- Gu, G., et al. (1989), *Catalogue of Chinese Earthquakes (1831 BC–1969 AD)*, Science Press, Beijing.
- He, W., et al. (2007), Paleo-earthquake study on the Maqu fault of East Kunlun Active Fault, *Earthquake Res. China*, in press.
- Hetzl, R., et al. (2002), Low slip rates and long term preservation of geomorphic features in central Asia, *Nature*, *417*, 428–432.
- Hilley, G. E., R. Bürgmann, P.-Z. Zhang, and P. Molnar (2005), Bayesian inference of plastosphere viscosities near the Kunlun Fault, northern Tibet, *Geophys. Res. Lett.*, *32*, L01302, doi:10.1029/2004GL021658.
- Holt, W. E., J. F. Ni, T. C. Wallace, and A. J. Haines (1991), The active tectonics of the Eastern Himalayan Syntaxis and surrounding regions, *J. Geophys. Res.*, *96*, 14,595–14,632.
- Houseman, G., and P. England (1993), Crustal thickening versus lateral expulsion in the Indian-Asian continental collision, *J. Geophys. Res.*, *98*, 12,233–12,249.
- Jolivet, M., M. Brunel, D. Seward, Z. Xu, J. Yang, J. Malavieille, F. Roger, A. Leyreloup, N. Arnaud, and C. Wu (2003), Neogene extension and volcanism in the Kunlun Fault Zone, northern Tibet: New constraints on the age of the Kunlun Fault, *Tectonics*, *22*(5), 1052, doi:10.1029/2002TC001428.
- Kidd, W. S. F., and P. Molnar (1988), Quaternary and active faulting observed on the 1985 Academia Sinica-Royal Society Geotraverse of Tibet, *Philos. Trans. R. Soc. London*, *327*, 337–363.
- King, R. W., et al. (1997), Geodetic measurement of crustal motion in southwest China, *Geology*, *25*, 179–182.
- Kirby, E., et al. (2000), Neotectonics of the Min Shan, China: Implications for mechanisms driving Quaternary deformation along the eastern margin of the Tibetan Plateau, *Geol. Soc. Am. Bull.*, *112*, 375–393.
- Li, H., et al. (2005), Slip rate on the Kunlun fault at Hongshui Gou, and recurrence time of great events comparable to the 14/11/2001, Mw ~ 7.9 Kokoxili earthquake, *Earth Planet. Sci. Lett.*, *237*, 285–299.
- Lin, A., et al. (2002), Co-seismic strike-slip and rupture length produced by the 2001 Ms 8.1 central Kunlun earthquake, *Science*, *296*, 2015–2017.
- Malservisi, R., T. H. Dixon, P. C. La Femina, and K. P. Furlong (2003), Holocene slip rate of the Wasatch fault zone, Utah, from geodetic data: Earthquake cycle effects, *Geophys. Res. Lett.*, *30*(13), 1673, doi:10.1029/2003GL017408.
- Mériaux, A.-S., F. J. Ryerson, P. Tapponnier, J. Van der Woerd, R. C. Finkel, X. Xu, Z. Xu, and M. W. Caffee (2004), Rapid slip along the central Altyn Tagh Fault: Morphochronologic evidence from Cherenchen He and Sulamu Tagh, *J. Geophys. Res.*, *109*, B06401, doi:10.1029/2003JB002558.
- Mériaux, A.-S., et al. (2005), The Aksay segment of the northern Altyn Tagh fault: Tectonic geomorphology, landscape evolution, and Holocene slip rate, *J. Geophys. Res.*, *110*, B04404, doi:10.1029/2004JB003210.
- Meyer, B., et al. (1996), Rate of left-lateral movement along the easternmost segment of the Altyn Tagh fault, east of 96°E (China), *Geophys. J. Int.*, *124*, 29–44.
- Molnar, P., and H. Lyon-Caen (1989), Fault plane solutions of earthquakes and active tectonics of the Tibetan Plateau and its margins, *Geophys. J. Int.*, *99*, 123–153.
- Molnar, P., and P. Tapponnier (1975), Cenozoic tectonics of Asia: Effects of a continental collision, *Science*, *189*, 419–426.
- Peacock, D. C. P. (1991), Displacements and segment linkage in strike-slip fault zones, *J. Struct. Geol.*, *13*, 1025–1035.
- Peltzer, G., and F. Saucier (1996), Present-day kinematics of Asia derived from geologic fault rates, *J. Geophys. Res.*, *101*, 27,943–27,956.
- Peltzer, G., P. Tapponnier, Z. Zhang, and Z. Q. Xu (1985), Neogene and Quaternary faulting in and along the Qinling Shan, *Nature*, *317*, 500–505.
- Peltzer, G., et al. (1999), Evidence of nonlinear elasticity of the crust from the Mw 7.6 Manyi (Tibet) earthquake, *Science*, *286*, 272–276.
- Royden, L. H., B. C. Burchfiel, R. W. King, E. Wang, Z. Chen, F. Shen, and Y. Liu (1997), Surface deformation and lower crustal flow in eastern Tibet, *Science*, *276*, 788–790.
- Savage, J. C., and R. O. Burford (1973), Geodetic determination of the relative plate motion in central California, *J. Geophys. Res.*, *78*, 832–845.
- Shen, Z.-K., J. Lü, M. Wang, and R. Bürgmann (2005), Contemporary crustal deformation around the southeast borderland of the Tibetan Plateau, *J. Geophys. Res.*, *110*, B11409, doi:10.1029/2004JB003421.

- Sieh, K. E., and R. H. Jahns (1984), Holocene activity of the San Andreas fault at Wallace Creek, California, *Geol. Soc. Am. Bull.*, *95*, 883–896.
- Stirling, M. W., et al. (1996), Fault trace complexity, cumulative slip, and the shape of the magnitude-frequency distribution for strike-slip faults: A global survey, *Geophys. J. Int.*, *124*, 833–868.
- Stuiver, M., et al. (1998), INTCAL98 radiocarbon age calibration 24,000–0 cal BP, *Radiocarbon*, *40*, 1041–1083.
- Tapponnier, P., and P. Molnar (1977), Active faulting and tectonics in China, *J. Geophys. Res.*, *82*, 2905–2930.
- Tapponnier, P., G. Pelzer, and R. Armijo (1986), On the mechanics of the collision between India and Asia, in *Collision Tectonics*, edited by M. P. Coward and A. C. Ries, *Geol. Soc. Spec. Publ.*, *19*, 115–157.
- Tapponnier, P., et al. (2001), Oblique stepwise rise and growth of the Tibet Plateau, *Science*, *294*, 1671–1677.
- Van der Woerd, J., et al. (1998), Holocene left-slip rate determined by cosmogenic surface dating on the Xidatan segment of the Kunlun Fault (Qinghai, China), *Geology*, *26*, 695–698.
- Van der Woerd, J., et al. (2000), Uniform slip-rate along the Kunlun Fault: Implications for seismic behavior and large-scale tectonics, *Geophys. Res. Lett.*, *27*, 2353–2356.
- Van der Woerd, J., et al. (2002a), The 14 November 2001, Mw = 7.8 Kokoxili earthquake in northern Tibet (Qinghai Province, China), *Seismol. Res. Lett.*, *73*, 125–135.
- Van der Woerd, J., et al. (2002b), Uniform postglacial slip-rate along the central 600 km of the Kunlun Fault (Tibet), from ²⁶Al, ¹⁰Be, and ¹⁴C dating of riser offsets, and climatic origin of the regional morphology, *Geophys. J. Int.*, *148*, 356–388.
- Vilotte, J. P., et al. (1986), Numerical study of continental collision: Influence of boundary forces and an initial stiff inclusion, *Geophys. J. R. Astron. Soc.*, *84*, 279–310.
- Wang, Q., et al. (2001), Present-day crustal deformation in China constrained by Global Positioning System measurements, *Science*, *294*, 574–577.
- Weldon, R. J., and K. E. Sieh (1985), Holocene rate of slip and tentative recurrence interval for large earthquakes on the San Andreas fault in Cajon Pass, southern California, *Geol. Soc. Am. Bull.*, *96*, 793–812.
- Wells, D. L., and K. J. Coppersmith (1994), New empirical relationships among magnitude, rupture length, rupture width, rupture area, and surface displacement, *Bull. Seismol. Soc. Am.*, *84*, 974–1002.
- Wright, T. J., et al. (2004), InSAR observations of low slip rates on the major faults of western Tibet, *Science*, *305*, 236–240.
- Yin, A., and T. M. Harrison (2000), Geologic evolution of the Himalayan-Tibetan orogen, *Annu. Rev. Earth Planet. Sci.*, *28*, 211–280.
- Zhang, P.-Z., et al. (2004), Continuous deformation of the Tibetan Plateau from global positioning system data, *Geology*, *32*, 809–812.
- Zhang, Y. Q., et al. (1995), Active faulting in and along the Qinling range (China) inferred from SPOT imagery analysis and extrusion tectonics of south China, *Tectonophysics*, *243*, 69–95.

N. Harkins and E. Kirby, Department of Geosciences, Pennsylvania State University, University Park, PA 16802, USA. (ekirby@geosc.psu.edu)

C. Fan, X. Shi, and E. Wang, Institute for Geology, Chinese Academy of Sciences, Beijing, China.

D. Burbank, Department of Earth Science, University of California, Santa Barbara, CA 93110, USA.